

# A Novel Bis(*trans*-thiocyanate)iron(II) Spin-Transition Molecular Material with Bidentate Triaryltriazole Ligands and Its Bis(*cis*-thiocyanate)iron(II) High-Spin Isomer

Dunru Zhu,<sup>†</sup> Yan Xu,<sup>†</sup> Zhi Yu,<sup>†</sup> Zijian Guo,<sup>†</sup> Hai Sang,<sup>‡</sup> Tao Liu,<sup>§</sup> and Xiaozeng You<sup>\*†</sup>

Coordination Chemistry Institute, State Key Laboratory of Coordination Chemistry, National Laboratory of Solid State Microstructures, Nanjing University, Nanjing 210093, People's Republic of China, and Synchrotron Radiation Laboratory, Institute of High Energy Physics, Chinese Academy of Science, Beijing 100039, People's Republic of China

Received August 2, 2001. Revised Manuscript Received November 9, 2001

Two novel complexes *trans*-[Fe(MBPT)<sub>2</sub>(NCS)<sub>2</sub>] (**1**) and *cis*-[Fe(mMBPT)<sub>2</sub>(NCS)<sub>2</sub>] (**2**) have been synthesized and their structure characterized at 293 K by single-crystal X-ray crystallography [MBPT (or mMBPT) = 4-*p*(or *m*)-methylphenyl-3,5-bis(pyridin-2-yl)-1,2,4-triazole]. Complexes **1** and **2** are isomers, and **1** crystallizes in the triclinic space group *P*<sub>1</sub> with *Z* = 1, *a* = 9.120(3) Å, *b* = 9.2563(18) Å, *c* = 11.576(2) Å, α = 76.256(15)°, β = 76.405(18)°, γ = 84.983(19)°, and *V* = 922.1(4) Å<sup>3</sup> in contrast to **2** in the monoclinic space group *C*2/*c* with *Z* = 4, *a* = 21.851(3) Å, *b* = 13.4113(15) Å, *c* = 16.859(3) Å, β = 128.153(9)°, and *V* = 3885.0(9) Å<sup>3</sup>. Both complexes have a similar pseudo-octahedral [FeN<sub>6</sub>] core with the NCS<sup>-</sup> groups in the *trans* arrangement in **1** but *cis* in **2**. Variable-temperature magnetic susceptibility and IR spectral measurements reveal that **1** shows an abrupt high-spin ↔ low-spin (HS ↔ LS) transition centered at *T*<sub>1/2</sub> around 231 K, in contrast to **2** staying in a high-spin state in the observed temperature range of 75–300 K. The extended X-ray absorption fine structures (EXAFS) spectra confirm that the average Fe–N distance for the HS state in **1** is ≈0.2 Å longer than that of the LS state. Complex **1** represents the first spin-crossover iron(II) complex with triaryltriazole and *trans*-thiocyanate ligands.

## Introduction

It is well-known that some transition-metal compounds with an electronic configuration of 3d<sup>4</sup>–3d<sup>7</sup> in octahedral environments show a spin-crossover phenomenon between LS and HS states induced by temperature changing, pressure, or light irradiation.<sup>1–5</sup> Because of the potential applications of spin crossover in molecular electronics,<sup>4</sup> memory devices,<sup>6</sup> and information storage<sup>7</sup> or in certain biological systems,<sup>8</sup> much attention has been focused on the understanding of the key factors to accomplish spin-crossover systems and on the exploration of novel spin-crossover molecular materials. Among them, the iron(II) spin-crossover

compounds, in particular [FeL<sub>2</sub>(NCS)<sub>2</sub>] [L = phen, bipy, 4,4'-bis-1,2,4-triazole (btr), etc.], are one of the most notable systems.<sup>9,10</sup> A fine modification of ligands would generate an intermediate ligand field that in turn can provide conditions favoring spin conversion, depending on the balance between the ligand field and the mean spin pairing energy. For this purpose, we have recently synthesized some new triaryltriazole ligands<sup>11</sup> where it is possible for the ligand field to be shifted to the region of spin crossover for Fe<sup>II</sup> derivatives through substitutions in the phenyl ring of the triaryltriazole. In this paper, we report the syntheses, structures, magnetic properties, and spectroscopic characterization of the first spin-crossover iron(II) complex with triaryltriazole, *trans*-[Fe(MBPT)<sub>2</sub>(NCS)<sub>2</sub>] (**1**), and its homologous high-spin iron(II) complex, *cis*-[Fe(mMBPT)<sub>2</sub>(NCS)<sub>2</sub>] (**2**).

## Experimental Section

**Materials.** All chemicals used were of analytical grade. Solvents were purified by conventional methods. The ligand MBPT or mMBPT was prepared as described previously.<sup>11</sup>

\* To whom correspondence should be addressed.

<sup>†</sup> Coordination Chemistry Institute, State Key Laboratory of Coordination Chemistry, Nanjing University.

<sup>‡</sup> National Laboratory of Solid State Microstructures, Nanjing University.

<sup>§</sup> Chinese Academy of Science.

(1) Goodwin, H. A. *Coord. Chem. Rev.* **1976**, *18*, 293.

(2) Gütllich, P. *Struct. Bonding* **1981**, *44*, 83.

(3) König, E.; Ritter, G.; Kulshreshtha, S. K. *Chem. Rev.* **1985**, *4*, 19.

(4) Gütllich, P.; Hauser, A.; Spiering, H. *Angew. Chem., Int. Ed. Engl.* **1994**, *33*, 2024.

(5) Kahn, O. *Molecular Magnetism*; VCH: New York, 1993.

(6) Kahn, O. *Chem. Britain* **1999**, Feb, 24.

(7) Kahn, O.; Martinez, C. J. *Science* **1998**, *279*, 44.

(8) Ficher, M. T.; Sligar, S. G. *Biochemistry* **1987**, *26*, 4797.

(9) Zhuang, J. Z.; Tao, J. Q.; Yu, Z.; Duan, C. Y.; Liu, Y. J.; You, X. Z. *J. Chem. Soc., Dalton Trans.* **1998**, 327 and references therein.

(10) Yu, Z.; Liu, K.; Tao, J. Q.; Zhuang, J. Z.; You, X. Z.; Siu, G. G. *Appl. Phys. Lett.* **1999**, *74*, 4029.

(11) Zhu, D. R.; Song, Y.; Xu, Y.; Zhang, Y.; Raj, S. S. S.; Fun, H. K.; You, X. Z. *Polyhedron* **2000**, *19*, 2109 and references therein.

**Characterization.** Elemental analyses of C, H, and N were determined on a Perkin-Elmer 240C elemental analyzer. The infrared spectra were recorded on a Nicolet-170SX FT-IR spectrometer with KBr pellets in the range 4000–400  $\text{cm}^{-1}$ . Electrospray ionization mass spectra (ESI-MS) were recorded with a Finnigan mat APISSQ 710 mass spectrometer, with MeOH as the mobile phase; the flow rate of the mobile phase was 0.2  $\text{cm}^3\cdot\text{min}^{-1}$ . The spray voltage was 4.5 kV and the capillary temperature 200 °C. The capillary voltage was 7.3 V for **1** and 28.7 V for **2**. Magnetic susceptibilities of the microcrystalline of **1** and **2** were collected using a CAHN 2000 magnetobalance in the temperature range of 75–300 K. The applied magnetic field was 0.7 T and the data were corrected for diamagnetism using Pascal's constants. The variable temperature infrared spectra of **1** were recorded on a Bruker IFS 66V FT-IR spectrometer in a poly(vinyl alcohol) film. The EXAFS experiments for **1** were carried out in transmission mode on the beam 4W1B at Beijing Synchrotron Radiation Faculty (BSRF), with the storage ring providing 2.2 GeV. The electron beam was 50–90 mA. A Si(111) double-crystal monochromator was used with the entrance slit at 0.5 mm. The spectra were recorded from 6906 to 7898 eV. The energy scale at the iron K edge was calibrated with reference to the strong absorption peak of elemental iron at 7111.2 eV. Samples were well-pounded microcrystalline powders of a homogeneous thickness and mounted in a sample cell of an aluminum sheet 2-mm thick and  $2.5 \times 3 \text{ cm}^2$  in cross section in which a window  $4 \times 12 \text{ mm}^2$  had been cut. Care was taken to make the sample thickness as uniform as possible. The two open ends of the aluminum holder were sealed with Mylar film. The spectra were recorded at room temperature and 77 K in a nitrogen cryostat that was designed for X-ray absorption spectroscopy.

**Syntheses.** All the manipulations were carried out under an argon atmosphere. To a solution of KSCN (0.6 mmol) in anhydrous MeOH (5 mL) was added a solution of  $\text{FeSO}_4 \cdot 7\text{H}_2\text{O}$  (0.3 mmol) in MeOH (4 mL). The mixture was stirred for 15 min, decanted off, and filtered. The  $\text{K}_2\text{SO}_4$  precipitate was washed with 2 mL of anhydrous MeOH. The methanolic fractions containing  $\text{Fe}(\text{SCN})_2$  were collected and then were added dropwise to a solution of the corresponding ligand (0.6 mmol) in MeOH (8 mL). A microcrystalline product, which formed immediately, was filtered and washed with  $\text{H}_2\text{O}$  and dried under an argon stream to give the corresponding complex.

$[\text{Fe}(\text{MBPT})_2(\text{NCS})_2]$  (**1**) as a red-brown solid. Yield: 91%. (Found: C, 60.67; H, 4.21; N, 21.35.  $\text{C}_{40}\text{H}_{30}\text{FeN}_{12}\text{S}_2$  requires C, 60.15; H, 3.79; N, 21.05%). IR ( $\text{cm}^{-1}$ ):  $\nu$  (CN) 2068 vs;  $\nu$  (py ring) 1597 s, 1585 m, 1573 w;  $\delta$  (ph ring) 828 s, 795 s. ESI-MS:  $m/z$  740.1 (100); 649.0; 497.7; 458.7; 356.7; 314.3.

$[\text{Fe}(\text{mMBPT})_2(\text{NCS})_2]$  (**2**) as a red solid. Yield: 85%. (Found: C, 60.05; H, 3.98; N, 20.67.  $\text{C}_{40}\text{H}_{30}\text{FeN}_{12}\text{S}_2$  requires C, 60.15; H, 3.79; N, 21.05%). IR ( $\text{cm}^{-1}$ ):  $\nu$  (CN) 2064 vs;  $\nu$  (py ring) 1601 s, 1588 m, 1571 w;  $\delta$  (ph ring) 796 s, 695 s. ESI-MS:  $m/z$  740.2; 649.1; 497.8; 458.9 (100); 356.9; 314.3.

**X-ray Crystallography.** A suitable single crystal of each complex was carefully selected under a polarizing microscope and glued to a thin glass fiber with adhesive. The crystal data were collected at 293 K on a Siemens P4 four-circle diffractometer with monochromated Mo  $K\alpha$  radiation ( $\lambda = 0.71073 \text{ \AA}$ ) using the  $\omega$ - $2\theta$  scan mode with a variable scan speed of  $4.0^\circ$ – $40.0^\circ \text{ min}^{-1}$  in  $\omega$ . The data were corrected for Lorentz and polarization effects during data reduction using XSCANS. The structure was solved by the direct methods and refined on  $F^2$  by full-matrix least-squares methods using SHELXTL version 5.10.<sup>12</sup> All non-hydrogen atoms were refined anisotropically. All hydrogen atoms were placed in calculated positions (C–H, 0.96 Å, and N–H, 0.90 Å), assigned fixed isotropic thermal parameters at 1.2 times the equivalent isotropic  $U$  of the atoms to which they are attached, and allowed to ride on their respective parent atoms. The contribution of these hydrogen

**Table 1.** Summary of Crystal Data for Complexes **1** and **2**

	complexes	
	<b>1</b>	<b>2</b>
empirical formula	$\text{C}_{40}\text{H}_{30}\text{FeN}_{12}\text{S}_2$	$\text{C}_{40}\text{H}_{30}\text{FeN}_{12}\text{S}_2$
$M_r$	798.73	798.73
temperature (K)	293(2)	293(2)
crystal size (mm)	$0.30 \times 0.21 \times 0.18$	$0.60 \times 0.56 \times 0.40$
crystal color, shape	red-brown, block	red, block
crystal system	triclinic	monoclinic
space group	$P\bar{1}$	$C2/c$
$a$ (Å)	9.120(3)	21.851(3)
$b$ (Å)	9.2563(18)	13.4113(15)
$c$ (Å)	11.576(2)	16.859(3)
$\alpha$ (deg)	76.256(15)	~
$\beta$ (deg)	76.405(18)	128.153(9)
$\gamma$ (deg)	84.983(19)	~
$V$ (Å <sup>3</sup> )	922.1(4)	3885.0(9)
$Z$	1	4
$D_c$ ( $\text{mg m}^{-3}$ )	1.438	1.362
$F(000)$	412	1648
$\mu$ ( $\text{mm}^{-1}$ )	0.571	0.542
diffractometer/scan	Siemens P4/ $\theta$ - $2\theta$	Siemens P4/ $\theta$ - $2\theta$
$\theta$ range (deg)	1.86–25.00	1.95–25.01
$hkl$	–1,10/–10,10/–13,13	–1,25/–1,15/–20,16
reflns collected	3902	4052
independent reflns	3226 ( $R_{\text{int}} = 0.1048$ )	3412 ( $R_{\text{int}} = 0.0367$ )
data/restraints/params	3226/0/247	250
GOF on $F^2$	1.029	1.015
R, wR indices ( $I > 2\sigma(I)$ )	0.0541, 0.1372	0.0697, 0.1789
R, wR indices (all data)	0.0741, 0.1513	0.1320, 0.2265
largest peak and hole ( $\text{e \AA}^{-3}$ )	0.575 and –0.796	0.315 and –0.318

**Table 2.** Selected Bond Distances (Å) and Angles (deg) for **1** and **2**

	<b>1</b>	<b>2</b>		<b>1</b>	<b>2</b>
Fe–N(6)	2.114(3)	Fe–N(5)	2.051(3)		
Fe–N(1)	2.213(3)	Fe–N(1)	2.217(2)		
Fe–N(2)	2.192(2)	Fe–N(2)	2.248(3)		
S(1)–C(20)	1.622(3)	S(1)–C(19)	1.586(4)		
N(6)–(20)	1.162(4)	N(5)–C(19)	1.154(5)		
C(19)–C(16)	1.506(4)	C(14)–C(20)	1.439(10)		
		C(16)–C(20A)	1.457(13)		
Fe–N(6)–C(20)	148.3(3)	Fe–N(5)–C(19)	164.5(3)		
N(6)–Fe–N(2)	94.52(11)	N(5)–Fe–N(2)	92.66(12)		
N(6)–Fe–N(1)	95.30(12)	N(5)–Fe–N(1)	97.34(9)		
N(1)–Fe–N(2)	74.17(10)	N(1)–Fe–N(2)	73.03(9)		
N(6)–C(20)–S(1)	179.3(3)	N(5)–C(19)–S(1)	178.2(4)		
N(6)–Fe–N(6) <sup>a</sup>	180.0(2)	N(5)–Fe–N(5) <sup>b</sup>	102.13(18)		
N(1)–Fe–N(1) <sup>a</sup>	180.00(12)	N(1)–Fe–N(1) <sup>b</sup>	163.24(13)		
N(2)–Fe–N(2) <sup>a</sup>	180.00(13)	N(2)–Fe–N(2) <sup>b</sup>	75.72(15)		

<sup>a</sup> Symmetry codes:  $-x, -y, -z$ . <sup>b</sup>  $-x, y, 1/2 - z$ .

atoms was included in the structure factor calculations. All computations were carried out on a PC-586 computer using the SHELXTL-PC program package. Analytical anomalous dispersion corrections were incorporated. Crystallographic data for **1** and **2** are summarized in Table 1. The selected bond distances and angles for **1** and **2** are presented in Table 2.

## Results and Discussion

**Syntheses.** The triaryltriazole ligand MBPT(or mMBPT) reacts with  $\text{FeSO}_4 \cdot 7\text{H}_2\text{O}$  and KNCS in molar ratio 2:1:2 to form a neutral monomeric hexacoordinate complex of formula  $[\text{FeL}_2(\text{NCS})_2]$  (L = MBPT or mMBPT), which is stable in air. Yields for complexes **1** and **2** are 91 and 85%, respectively. The elemental analysis was satisfactory and indicates that each complex contains one iron atom, two triaryltriazole ligands, and two thiocyanate groups.

**Crystal Structures.** The crystal, suitable for X-ray diffraction, was obtained by evaporation from a metha-

(12) Sheldrick, G. M. SHELXTL, Structure Determination Software Programs, Version 5.10; Bruker Analytical X-ray Systems Inc.; Madison, WI, 1997.

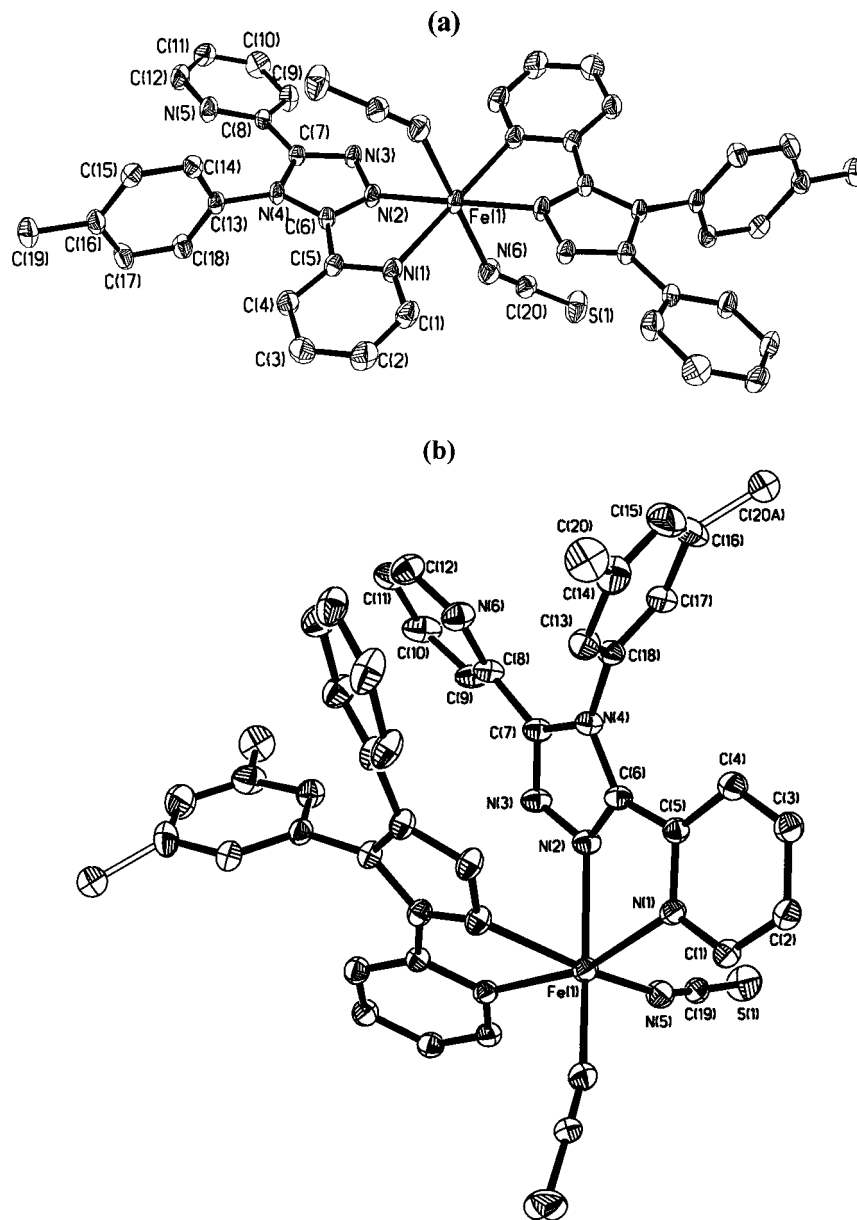


**Figure 1.** ORTEP view of complexes: (a) for **1** and (b) for **2** (H atoms omitted for clarity; thermal ellipsoids are at the 30% probability level).

nol solution. Complex **1** crystallizes in the triclinic space group  $P\bar{1}$ . Figure 1a shows the principal structural features with the atom-labeling scheme, and Table 2 gives the bond distances and angles relevant to the iron coordination spheres. The crystal structure of **1** shows that there is an inversion center at the iron(II) atom. Each iron atom is octahedrally coordinated to four nitrogen atoms from two triaryltriazole ligands (MBPT) and nitrogen atoms of two  $\text{NCS}^-$  ions in a trans arrangement. The octahedron geometry is distorted, as  $\text{Fe}-\text{N}(\text{CS})$  bond lengths [2.114(3) Å] are shorter than  $\text{Fe}-\text{N}(\text{MBPT})$ . The  $\text{Fe}-\text{N}(\text{MBPT})$  lengths also differ considerably for different nitrogen ligands [2.192(2) Å for triazole and 2.213(3) Å for pyridine]. The  $\text{NCS}$  groups are almost linear [ $\text{N}(6)-\text{C}(20)-\text{S}(1)$  179.3(3)°], whereas the  $\text{Fe}-\text{NC}(\text{S})$  linkages are rather bent [ $\text{Fe}-\text{N}(6)-\text{C}(20)$  148.3(3)°], which deviates even more far from 180° than in other analogous *trans*- $\text{NCS}^-$  iron(II) compounds, for instance, 153.7(3)° for  $[\text{Fe}(\text{btr})_2(\text{NCS})_2](\text{H}_2\text{O})$ <sup>13</sup> and 172.3(6)° for  $[\text{Fe}(\text{trans-stpy})_4(\text{NCS})_2]$  (stpy = 4-styrylpyri-

dine).<sup>14</sup> The ligand (MBPT) coordinates to the iron atom via the N(1) atom of a pyridyl ring and the N(2) atom of the triazole moiety, leaving the N(5) atom of another pyridyl ring and the N(3) atom of the triazole moiety uncoordinated, which is similar to the coordination mode in complexes  $[\text{M}(\text{MBPT})_2(\text{H}_2\text{O})_2](\text{ClO}_4)_2 \cdot n\text{H}_2\text{O}$  ( $\text{M} = \text{Co}^{\text{II}}$  and  $\text{Ni}^{\text{II}}$ ;  $n = 4$  or 0)<sup>11</sup> and  $[\text{Ag}(\text{MBPT})(\text{PPh}_3)_2]\text{ClO}_4$ .<sup>15</sup> It is noticeable that the  $\text{Fe}-\text{N}$  bond to the triazole nitrogen is 0.02 Å shorter than that to the pyridyl nitrogen. This feature can be compared with those features observed for complexes with 4-amino-3,5-bis(pyridin-2-yl)-1,2,4-triazole ligand (ABPT).<sup>16–20</sup> The ligand MBPT is nonplanar. The pyridyl ring where the

(13) Vreugdenhil, W.; Hassnoot, J. G.; Kahn, O.; Thuéry, P.; Reedijk, J. *J. Am. Chem. Soc.* **1987**, *109*, 5272.

(14) Roux, C.; Zarembowitch, J.; Gallois, B.; Granier, T.; Claude, R. *Inorg. Chem.* **1994**, *33*, 2273.

(15) Shao, S. C.; Zhu, D. R.; Zhu, X. H.; You, X. Z.; Raj, S. S. S.; Fun, H. K. *Acta Crystallogr.* **1999**, *C55*, 1412.

(16) Faulmann, C.; van Koningsbruggen, P. J.; de Graaff, R. A. G.; Haasnoot, J. G.; Reedijk, J. *Acta Crystallogr.* **1990**, *C46*, 2357.

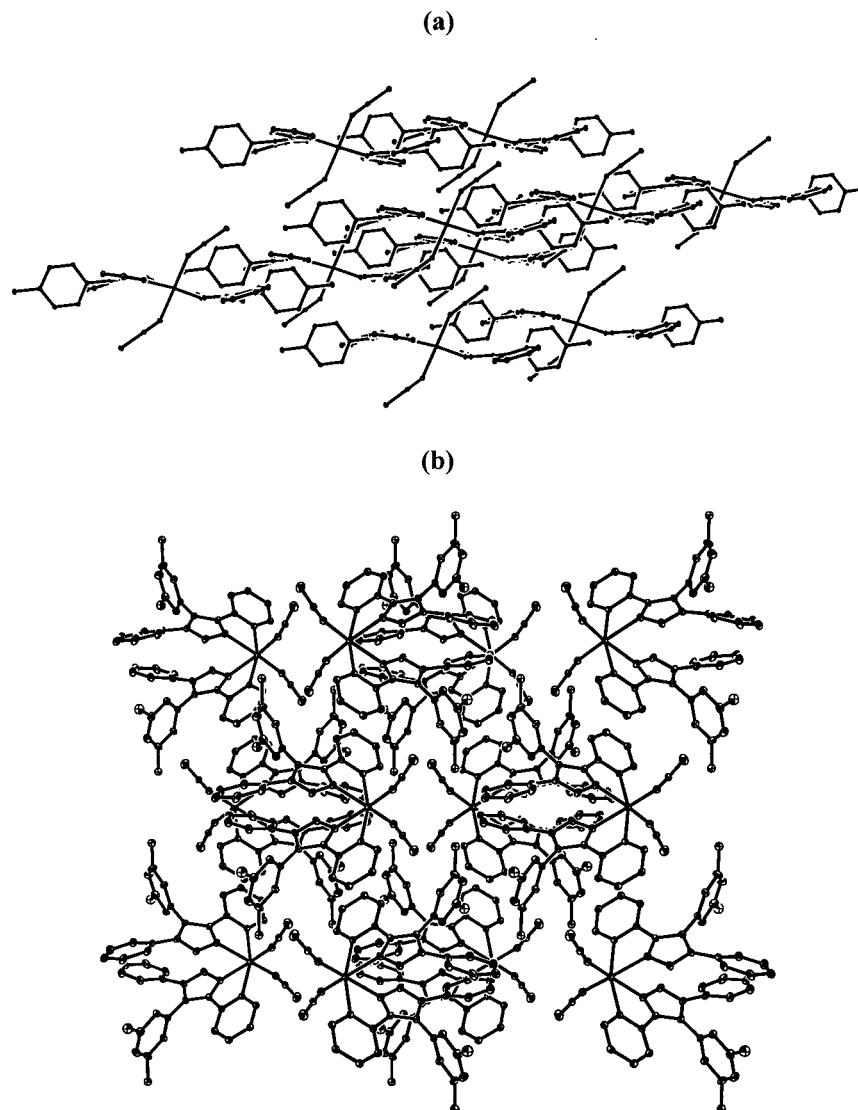


**Figure 2.** Structure of complexes projected along the *a* axis for **1** (a) and *c* axis for **2** (b).

nitrogen atom is involved in coordination makes an angle of  $11.6(3)^\circ$  with respect to the triazole ring, whereas the noncoordinating pyridyl ring makes an angle of  $14.8(3)^\circ$  with respect to the triazole plane. The same feature has been found in other mononuclear ABPT compounds. It is worthwhile to note that in the crystal structure of **1** the noncoordinating pyridyl ring and its symmetry-related partner (symmetric operation:  $1 - x, -1 - y, -z$ ) involve intermolecular  $\pi$ - $\pi$  stacking interactions with a separation of  $3.593(1)$  Å to stabilize the extended structure. These stacking interactions are presented in Figure 2a.

The structure of complex **2** is shown in Figure 1b, together with the atom-numbering scheme. Selected bond distances and angles are also given in Table 2. In this case there is a symmetric plane through the iron

atom. The iron atom is octahedrally coordinated to four nitrogen atoms from two mMBPT ligands and nitrogen atoms of two NCS<sup>-</sup> ions in cis arrangement. The octahedron is distorted, as Fe-N(CS) bond lengths  $2.051(3)$  Å are shorter than Fe-N (mMBPT)  $2.248(3)$  and  $2.217(2)$  Å. Moreover, the geometry constraints of the mMBPT ligand cause significant reduction of the N(1)-Fe-N(2) bond angle [ $73.09(9)^\circ$ ] from the ideal  $90^\circ$  value. This distortion of the FeN<sub>6</sub> core from *O<sub>h</sub>* symmetry is also observed in the high-spin phase structure of similar [FeL<sub>2</sub>(NCS)<sub>2</sub>] (L = phen or bipy) complexes.<sup>21,22</sup> The NCS groups are almost linear [N(5)-C(19)-S(1)  $178.2(4)^\circ$ ], whereas the Fe-NC(S) linkages are bent [Fe-N(5)-C(19)  $164.5(3)^\circ$ ]. It is worthwhile to mention that in the present structure the C atom of the methyl group is highly disordered. [The occupancy factors for C(20) and C(20A) are fixed as 0.73 and 0.27, respectively.] The crystal cohesion is achieved by van der Waals interactions. A stereo packing diagram is depicted in Figure 2b.

(17) Hartmann, U.; Vahrenkamp, H. *Inorg. Chim. Acta* **1995**, *239*, 13.

(18) Cornelissen, J. P.; van Diemen, J. H.; Groeneveld, L. R.; Haasnoot, J. G.; Spek, A. L.; Reedijk, J. *Inorg. Chem.* **1992**, *31*, 198.

(19) Kunkeler, P. J.; van Koningsbruggen, P. J.; Cornelissen, J. P.; van der Horst, A. N.; van der Kraan, A. M.; Spek, A. L.; Haasnoot, J. G.; Reedijk, J. *J. Am. Chem. Soc.* **1996**, *118*, 2190.

(20) van Koningsbruggen, P. J.; Goubitz, K.; Haasnoot, J. G.; Reedijk, J. *Inorg. Chim. Acta* **1998**, *268*, 37.

(21) Gallois, B.; Real, J. A.; Hauw, C.; Zarembowitch, J. *Inorg. Chem.* **1990**, *29*, 1152.

(22) Real, J. A.; Muñoz, M. C.; Andréz, E.; Granier, T.; Gallois, B. *Inorg. Chem.* **1994**, *33*, 3587.

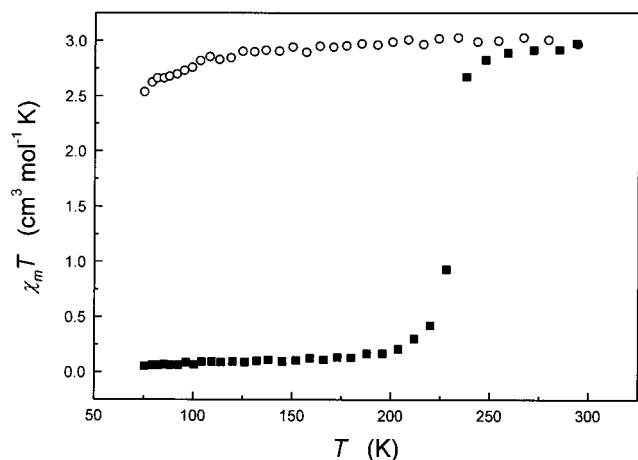


**Figure 3.** Thermal variation of  $\chi_m T$  for **1** (■) and **2** (○).

**Magnetic Properties.** The magnetic properties of **1** shown in Figure 3 reveal a relatively abrupt spin transition from the HS ( $S = 2$ ) to the LS ( $S = 0$ ) states compared with those related mononuclear iron(II) complexes.<sup>23</sup> At 293.6 K the magnitude of  $\chi_m T$  ( $2.97 \text{ cm}^3 \cdot \text{mol}^{-1} \cdot \text{K}$ ) in corresponding to a HS state slowly decreases upon cooling until 240 K, and then a sharp spin conversion occurs between 240 and 220 K within transition temperature  $T_{1/2}$  (temperature for which the high-spin fraction is equal to 0.5) being 231 K. At 75.4 K the  $\chi_m T$  reaches  $0.05 \text{ cm}^3 \cdot \text{mol}^{-1} \cdot \text{K}$ , which is close to the expected value of temperature-independent paramagnetism for LS iron(II) complexes. The agreement of the experimental  $\chi_m T$  value to the theoretical one of a pure LS state suggests that the transition is complete. The curve obtained by warming mode is identical to that by a cooling one, indicating no hysteresis loop in the transition. Compared with **1**, complex **2** retains a HS state in the entire observed temperature range and this behavior can be interpreted by Curie–Weiss law,  $\chi_m = C/(T - \theta)$ , with a Curie value of 3.33 and Weiss constant of  $-15.55 \text{ K}$ .

**EXAFS Spectra.** The spin transition of **1** is also demonstrated by the variable temperature EXAFS spectra. The magnitude of Fourier transforming of the  $k^3$ -multiplied EXAFS data for **1** at both 293 and 77 K is indicated in Figure 4, which shows the prominent contraction ( $\approx 0.2 \text{ \AA}$ ) of the first-coordination shell around the iron upon cooling from 293 to 77 K. This structural change is associated with transition from the high-spin state at 293 K to the low-spin state at 77 K for **1** with a simultaneous shortening ( $\approx 0.2 \text{ \AA}$ ) of the Fe–N distances and changes in N–Fe–N and Fe–N–(CS) angles.<sup>24</sup> This is consistent with those obtained for related spin-crossover iron(II) compounds.<sup>25</sup>

**Variable-Temperature IR.** The spin transition of **1** is also studied by IR spectroscopy in the range of 110–300 K. Selected spectra are plotted in Figure 5, focusing on a  $2000\text{--}2150\text{-cm}^{-1}$  frequency range that corresponds to the C≡N stretching vibration of the NCS ligands.<sup>26</sup>

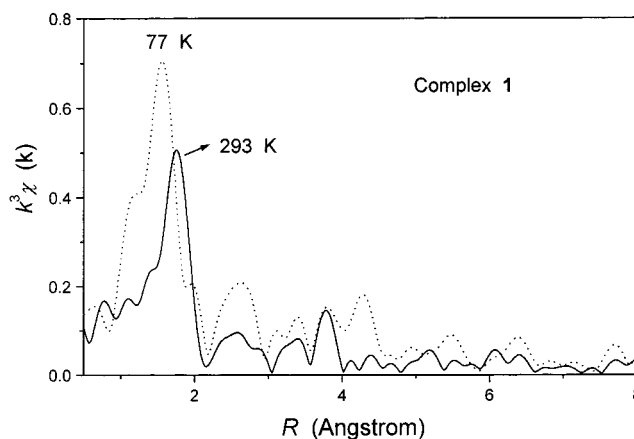


**Figure 4.** The Fourier transform of the  $k^3$ -multiplied EXAFS data for **1** at 293 and 77 K.

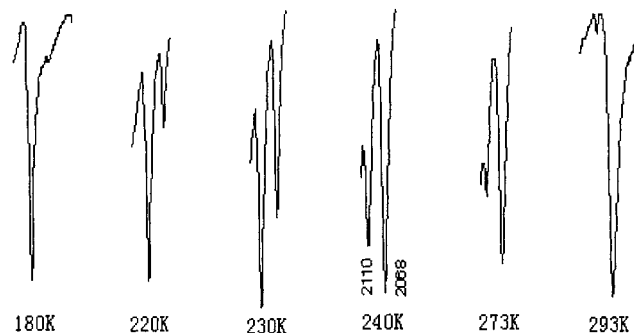


**Figure 5.** Temperature dependence of IR spectra of **1** in the region of  $2000\text{--}2150 \text{ cm}^{-1}$ .

The singlet ( $\approx 2068 \text{ cm}^{-1}$ ) observed mainly in a HS state at 293 K and ( $\approx 2110 \text{ cm}^{-1}$ ) in a LS state at low temperatures indicates two NCS ligands are in trans configuration in contrast to the splitting of this absorption for *cis*-[Fe(phen)<sub>2</sub>(NCS)<sub>2</sub>].<sup>26–31</sup> This is consistent with the results of X-ray analysis. Upon cooling from 293 K, the intensity of the singlet of  $2110 \text{ cm}^{-1}$  continuously increases and the intensity ratio of the two singlets is reversed approximately at  $T_c$ , revealing the spin transition behavior. Finally, at 180 K, the singlet of the HS state vanishes almost, in good agreement with magnetic studies. These spectral variations are highly reproducible as magnetic measurements show, but IR spectroscopy is more sensitive to the magnetic method while a very weak peak of the LS state in  $2110 \text{ cm}^{-1}$  associated with the HS state is recorded at 293 K.

Spin transition behaviors have been rarely observed in iron(II) complexes with trans-oriented NCS groups and, up to now, only four examples of such iron(II) spin-crossover complexes structurally characterized have been reported.<sup>14,32–34</sup> Complex **1** is the second example of bis(*trans*-thiocyanate)iron(II) spin-crossover com-

(23) Moliner, N.; Muñoz, M. C.; van Koningsbruggen, P. J.; Real, J. A. *Inorg. Chim. Acta* **1998**, *274*, 1.

(24) König, E. *Prog. Inorg. Chem.* **1987**, *35*, 527.

(25) Konno, M.; Mikami-Kido, M. *Bull. Chem. Soc. Jpn.* **1991**, *64*, 339.

(26) Baker, W. A., Jr.; Long, G. J. *J. Chem. Soc., Chem. Commun.* **1965**, 368.

(27) Biagini-Cingi, M.; Manotti-Lanfredi, A. M.; Tiripicchio, A.; Cornelissen, J. P.; Haasnoot, J. G.; Reedijk, J. *Inorg. Chim. Acta* **1987**, *127*, 189.

(28) Brooker, S.; Plioger, P. G.; Moubaraki, B.; Murray, K. S. *Angew. Chem., Int. Ed.* **1999**, *38*, 408.

(29) König, E.; Madeja, K. *Inorg. Chem.* **1967**, *6*, 48.

(30) Baldenius, K. U.; Campen, A. K.; Höhnk, H. D.; Rest, A. J. *J. Mol. Struct.* **1987**, *157*, 295.

(31) Coronel, P.; Barraud, A.; Claude, R.; Kahn, O.; Teixier, A. R.; Zarembowitch, J. *J. Chem. Soc., Chem. Commun.* **1989**, 193.

(32) Real, J. A.; Andr ez, E.; Muñoz, M. C.; Julve, M.; Granier, T.; Bousseksou, A.; Varret, F. *Science* **1995**, *268*, 265.

plexes with two bidentate ligands. Compared with the first example,  $[\text{Fe}(\text{ABPT})_2(\text{NCS})_2]$ , complex **1** shows more abrupt spin conversion. This abruptness is due to the cooperativity in the solid state, which may result from the existence of  $\pi$ - $\pi$  stacking interaction<sup>4,9,32</sup> and the introduction of a substituted phenyl group to the ABPT ligand. Moreover, the abrupt spin transition at 231 K in **1** is the highest critical temperature in the family of *trans*- $[\text{FeL}_2(\text{NCS})_2]$  complexes.

The late Kahn pointed out the five requirements of a spin-crossover compound that must be fulfilled to be used for data recording; they are abruptness, hysteresis, room temperature, change of color, and chemical stability.<sup>35</sup> Although the spin transition of **1** does not show any hysteresis, the abrupt completed spin conversion

at a relatively high temperature make **1** be potentially useful as molecular switching materials.

It is also interesting to note that the position of the methyl in MBPT and mMBPT ligands leads to a dramatic change in the crystal structure: *trans*-oriented  $\text{NCS}^-$  in **1** but *cis* in **2**. Moreover, the great differences between the structures of **1** and **2** also result in a prominent discrepancy in their magnetic properties: spin crossover for **1** and high spin for **2**. Further studies on the origin of the change in the crystal field responsible for this result are currently in progress.

**Acknowledgment.** This work was funded by the Major State Basic Research Development Program (Grant G2000077500) and the National Nature Science Foundation of China.

**Supporting Information Available:** Tables of crystal data, structure solution and refinement, atomic coordinates, bond lengths and angles, and anisotropic thermal parameters for **1** and **2** (PDF and CIF). This material is available free of charge via the Internet at <http://pubs.acs.org>.

CM010688U

(33) Vreugdenhil, W.; van Diemen, J. H.; De Graaff, R. A. G.; Haasnoot, J. G.; Reedijk, J.; Kahn, O.; Zarembowitch, J. *Polyhedron* **1990**, *9*, 2971.

(34) Moliner, N.; Muñoz, M. C.; Létard, S.; Létard, J.-F.; Solans, X.; Burriel, R.; Castro, M.; Kahn, O.; Real, J. A. *Inorg. Chim. Acta* **1999**, *291*, 279.

(35) Kahn, O.; Kröber, J.; Jay, C. *Adv. Mater.* **1992**, *4*, 718.